Cement and Concrete Composites 104 (2019) 103359

Contents lists available at ScienceDirect

Cement and Concrete Composites

journal homepage: www.elsevier.com/locate/cemconcomp

Characterization of viscoelastic behavior of synthetic alkali–silica reaction gels

Asghar Gholizadeh-Vayghan[a,b], Farshad Rajabipour[c,*], Mehran Khaghani[d], Michael Hillman[e]

[a] Department of Civil Engineering, K.N.Toosi University of Technology, Tehran, Iran
[b] Flemish Institute for Technological Research (VITO), Mol, Belgium
[c] Department of Civil and Environmental Engineering, Pennsylvania State University, 231M Sackett Building, University Park, PA, 16802, USA
[d] Geneva School of Economics and Management, University of Geneva, Switzerland
[e] Department of Civil and Environmental Engineering, Pennsylvania State University, University Park, PA, USA

ARTICLE INFO

Keywords:
Alkali – Silica reaction
Viscoelasticity
Mechanical properties
Characterization
Statistical modeling

ABSTRACT

The viscoelastic properties of ASR gels have a major impact on the gels' restrained swelling pressure and the resulting damage to concrete. This study employed a design of experiments approach to synthesize and test eighteen cylindrical ASR gel specimens of different compositions, expressed in terms of their Ca/Si, Na/Si and K/Si molar ratios. The gel cylinders were loaded uniaxially to determine their compressive strength and Poisson's ratio. In addition, the true stress – strain – time results under constant load were used, in combination with the Burgers model, to extract the viscoelastic parameters of the gels, including elastic moduli and viscosity values. These were linked to the gels' chemical composition via regression analyses. It was observed that gels with higher alkali contents had drastically reduced elastic moduli and viscosity. In contrast, the concentration of calcium in the gels generally increased such mechanical properties.

1. Introduction

Interest in computer modeling of expansion and damage caused by the alkali-silica reaction (ASR) in concrete has been growing due to the potential utility of such models for predicting the service-life of new and existing structures, and for optimizing the type and timing of repairs [1–8]. While accelerated laboratory tests have been unable to quantitatively predict the field ASR performance of structures over a long term [9], integration of such test results with computer models can provide a much-needed breakthrough in service-life modeling of ASR-susceptible structures.

For these models to be reliable, they must employ an accurate knowledge of the mechanical and swelling behavior and material properties of ASR gels as a function of gel compositions. For example, the viscoelastic nature and response of ASR gels under confining stress have a major impact on the swelling stress that the gels can generate inside concrete, and the rate of stress attenuation over time. The bulk elastic modulus of ASR gels, which represents their compressibility, also affects the extent of stress and damage that they can cause. ASR gels can also flow under the confining stress; as such, more flowable gels, characterized by their low yield strength, are less deleterious [12]. Other significant properties of ASR gels are their hydrophilic potential, free swelling capacity, and restrained swelling pressure. In our previous works, we have successfully established quantitative composition-property relationships for ASR gels for their hydrophilic potential [10], swelling capacity and swelling pressure [11], and rheological properties [12]. In this paper, we intend to expand this approach by linking the composition and mechanical properties of ASR gels; namely, their viscoelastic parameters, compressive strength, and Poisson's ratio.

The majority of existing ASR damage models only consider the elastic (and not the viscous) response of ASR gels [13]. They use elastic modulus values that were obtained from a limited number of direct measurements on silica gels [14,15], or those that were estimated indirectly based on micro – indentation [16] or X – ray absorption and Brillouin spectroscopy measurements [14]. The elastic modulus values reported for synthetic silica gels range from 14 to 49 GPa, depending on the gels' solid concentration [15]. Micro – indentation suggested the elastic modulus of "ASR products" to be in the range 5–10 GPa [16], while the X – ray absorption techniques suggested a bulk modulus of ASR products to be as high as 33 GPa, which translates to an elastic modulus of 59 GPa, assuming a Poisson's ratio of 0.2. Besides the high variability in the reported values, there are additional problems with using such elastic modulus values in ASR damage models: (1) These measurements either correspond to synthetic "silica gels" (with

* Corresponding author.
E-mail address: fxr10@psu.edu (F. Rajabipour).

https://doi.org/10.1016/j.cemconcomp.2019.103359
Received 12 July 2018; Received in revised form 31 May 2019; Accepted 27 June 2019
Available online 29 June 2019
0958-9465/

Table 1
The experimented levels of different composition variables of ASR gels.

Coded levels	Categorical	Low (L)	Intermediate Low (IL)	Intermediate (I)	Intermediate High (IH)	High (H)
	Numerical	−1.68	−1	0	+1	+1.68
Test variables		Corresponding natural levels (molar ratios)				
Ca/Si: C		0.05	0.141	0.275	0.409	0.5
Na/Si: N		0.1	0.282	0.55	0.818	1.0
K/Si: K		0.0	0.061	0.15	0.239	0.3

chemical compositions very different than those of ASR gels) or "ASR products"; i.e., what is deemed to be ASR gel in fractured concrete specimens, which is not solely ASR gel, but often mixed with aggregate fragments and hydration products. (2) The test methods for determination of the elastic modulus were indirect in the case of micro−-indentation and X−ray absorption. (3) The ASR product samples were subject to carbonation and moisture changes during handling and testing, which can drastically alter the test results and gel properties. (4) The obtained results only apply to specific ASR gel compositions and fail to take into account the effects of composition on properties of gels. (5) The tested field ASR products may have been old and as such, had already undergone alkali−recycling and densification, which reduced their swelling and deleteriousness [10,17,18]. (6) The test methods used for measuring or estimating the elastic modulus assumed a simple elastic response for ASR gels, while they actually show viscoelastic deformation during testing; and this can compromise the validity of the measured elastic modulus [16]. Moreover and as stated earlier, the time-dependent (viscoelastic) response of ASR gels to stress and its dependence on the gel composition must be accounted for within the damage models. Unfortunately, such information is currently unavailable, resulting in high inaccuracies in modeling predictions.

The present study pursues two objectives: (1) to measure the compressive strength, Poisson's ratio, and viscoelastic parameters (including elastic modulus and viscosity values) of ASR gels under uniaxial loading; and (2) to relate such properties to the composition of ASR gels. A robust design of experiments (DoE) and statistical model was developed that can be used to estimate the viscoelastic parameters of ASR gels with known reliability and as a function of the gels' chemical composition.

2. Experimental program

2.1. Materials

ASR gels are silica-based hydrogels incorporating varying amounts of alkali and alkaline earth oxides (primarily sodium, potassium, and calcium oxides) [19]. Their general chemical composition can be represented as $(SiO_2)(CaO)_c(Na_2O)_n(K_2O)_k(H_2O)_x$, where the molar ratios c, n, k, and x are subject to variations with time, space, and composition of the host aggregate and concrete. Synthetic ASR gels can be produced by carefully combining and mixing certain precursor materials to match the target composition of ASR gels. The method used in this study for synthesizing the ASR gels are described here. Dried, pulverized colloidal silicon dioxide IV (50% H_2O, procured from Alfa Aesar) with an average particle size of 6.37 μm was used as the source of amorphous silica. The colloidal silica was dried to constant mass at 110 °C for 48 h, followed by 48 h of grinding inside a 5−Lit porcelain jar mill. The source of silica contained an initial Na/Si atomic ratio of 0.022, which was taken into account in calculating the required NaOH content for synthesizing each ASR gel. $Ca(OH)_2$ powder (assay: > 95%) was used as the source of calcium. NaOH and KOH pellets (99% assay) were used as the sources of sodium and potassium. The chemically-bound water in $Ca(OH)_2$, NaOH and KOH was subtracted from the total mixing water needed to reach the target moisture content of the gels (40% by mass). More details on ASR gel synthesis are provided below and in Ref. [10].

2.2. Methods

2.2.1. Design of experiments (DoE)

Similar to our previous works [10,11], the ranges of gel compositions studied in this work were as follow: Ca/Si = (0.05–0.5), Na/Si = (0.1–1.0), and K/Si = (0.0–0.3) molar ratios. These ranges were chosen based on the outcomes of a statistical analysis performed on the chemical compositions of 100 different field ASR gel samples reported in the literature, and also the ranges suggested by Hou et al. [19]. These ranges were concluded to cover the vast majority of all ASR gel compositions as they form in concrete, and as such, were studied here to obtain a full picture of the effects of composition on the mechanical and viscoelastic properties of ASR gels. The experiments were designed based on the concepts of the central composite design [20] in order to enable statistical assessment of the linear and nonlinear effects, and interactions of ASR gels' composition variables (Ca/Si, Na/Si and K/Si) on their properties (compressive strength, Poisson's ration, and viscoelastic parameters). To that end, each composition variable was studied at five distinct levels as shown in Table 1.

ASR gels with 15 different compositions as shown in Table 2 were synthesized. Their moisture content was held constant at 40%. The gels were labeled based on the levels of their composition variables. For instance, $C^{IH}N^{IH}K^{IL}$ denotes a gel with its Ca/Si at the intermediate−high (IH) level (i.e., 0.409 as suggested by Table 1), Na/Si at the intermediate−high level (0.818) and K/Si at the intermediate−low (IL) level (0.061). After designing the experiments, the run order was randomized to eliminate the effects of testing time on the results. Following the concepts of the central composite design, four identical gels with $C^{I}N^{I}K^{I}$ composition were produced and tested as replicates in order to increase the power of the statistical analyses.

2.2.2. Synthesis of ASR gels

A temperature−controlled high−shear mixing protocol was developed for batching the gels. First, the alkalis (KOH and NaOH) were dissolved in distilled water and stored at 1 °C. The silica and calcium hydroxide powders were dry−blended and stored at −18 °C. After 3 h, the alkaline solution and powder blend were removed from the cold storage and mixed as follows. The alkaline solution was first transferred to a cylindrical PVC container and the powder was immediately added to the solution. Using a hand−held drill equipped with a tri−blade paddle, the materials were mixed at 60–100 rpm for 15 s or until the contents converted to a consistent paste. Then, the paste was mixed at 1000 to 1500 rpm for 90 s to obtain a fully homogeneous paste. The obtained mixture was transferred into 5 × 10 cm cylindrical molds, sealed, and after two days, demolded and vacuum sealed-cured for two months. This was to ensure the completion of gelation reactions before

Table 2
Chemical compositions and mixture proportions[a] of the synthesized ASR gels.

Run order	Label	Ca/Si	Na/Si	K/Si	$Ca(OH)_2$	NaOH	KOH	Silica[b]	H_2O
1	$C^{IL}N^{IH}K^{IH}$	0.141	0.818	0.239	60.0	182.7	76.9	348.4	331.9
2	$C^{IL}N^{IL}K^{IH}$	0.141	0.282	0.239	71.3	71.1	91.4	414.2	352.0
7, 11, 12, 15	$C^{I}N^{I}K^{I}$ (1) to (4)	0.275	0.550	0.150	122.7	127.4	50.7	365.9	333.4
3	$C^{I}N^{L}K^{I}$	0.275	0.100	0.150	142.7	21.9	58.9	425.6	350.9
4	$C^{IL}N^{IL}K^{IL}$	0.141	0.282	0.061	78.8	78.6	25.7	457.9	359.0
5	$C^{H}N^{I}K^{I}$	0.500	0.550	0.150	198.0	113.0	45.0	324.8	319.2
6	$C^{I}N^{H}K^{I}$	0.275	1.000	0.150	107.6	206.9	44.4	320.9	320.1
8	$C^{IH}N^{IL}K^{IH}$	0.409	0.282	0.239	176.4	60.7	78.1	353.9	330.9
9	$C^{IH}N^{IH}K^{IH}$	0.409	0.818	0.239	151.9	159.8	67.3	304.7	316.3
10	$C^{I}N^{I}K^{H}$	0.275	0.550	0.300	114.6	118.9	94.6	341.7	330.2
13	$C^{L}N^{I}K^{I}$	0.050	0.550	0.150	25.5	145.8	58.0	419.0	351.7
14	$C^{IH}N^{IH}K^{IL}$	0.409	0.818	0.061	163.4	171.9	18.4	327.7	318.6
16	$C^{IL}N^{IH}K^{IL}$	0.141	0.818	0.061	65.2	198.7	21.3	378.8	336.0
17	$C^{IH}N^{IL}K^{IL}$	0.409	0.282	0.061	192.1	66.1	21.6	385.3	334.9
18	$C^{I}N^{I}K^{L}$	0.275	0.550	0.000	132.1	137.1	0.0	393.8	337.0

[a] The masses of the chemical components are in grams per each 1000 g of gel.
[b] Dried, pulverized colloidal silica as described in Section 2.1.

measuring the mechanical properties of ASR gels as described in the next section.

2.2.3. Compressive strength measurement

The rationale behind testing the gels for their compressive strength was to determine the uniaxial stress magnitude that should be applied to each gel specimen during the measurement of its viscoelastic properties. For creep testing of concrete, ASTM C512 suggests applying a uniaxial stress value equal to 40% of the specimen's compressive strength to maintain a linear creep behavior. Linear creep means that the magnitude of creep strain is proportional with that of elastic strain, independent of the value of applied stress. In this study, we adopted the same approach and applied a uniaxial stress at 40% level of each gel's compressive strength. We assumed creep linearity; however, this assumption should be validated in future research by testing ASR gels at various stress levels to determine if the obtained viscoelastic parameters are stress dependent. For the compressive strength measurements, loading was applied using an 11-kip (49 KN) MTS servo-hydraulic loading frame at a rate that would lead to failure of the specimen in 1–2 min.

2.2.4. Poisson's ratio measurements

The Poisson's ratios of the gels were measured using an ASTM C469 compressometer suited for 5 × 10 cm specimens (Fig. 1.). The compressometer was placed around and attached to each gel specimen using two diametrically opposed studs. The specimen was loaded at a constant rate up to $0.4\sigma_c$ and the radial strain was measured using the dial gage with an accuracy of 0.025 mm. Poisson's ratio was calculated as negative of the ratio of the radial to longitudinal strains. The radial displacement was tracked over time during the experiments and was observed to be linearly proportional with the longitudinal strain. The Poisson's ratio was therefore time-independent.

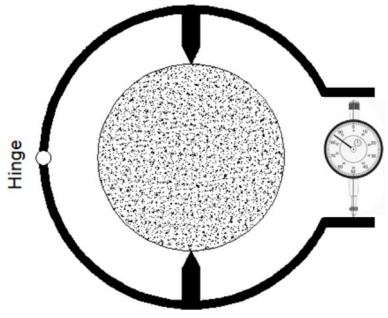

Fig. 1. Schematics of the compressometer used for the Poisson's ratio measurement of ASR gels.

2.2.5. Viscoelastic properties measurements

One 5 × 10 cm cylindrical specimen was cast and cured for testing each gel for its viscoelastic properties and Poisson's ratio. The specimens were uniaxially loaded up to a stress level of $0.4\sigma_c$ (i.e., 40% of their compressive strength) in approximately 30 s. Teflon sheets were used at the top and bottom of each cylinder to serve as roller supports and ensure true uniaxial state of stress. In addition, cylinders were covered with paraffin wax tape to prevent drying and formation of capillary stresses that would result in an uncontrolled tri − axial state of stress.

The uniaxial compressive load was held constant at $0.4\sigma_c$ for a sufficient duration of time to collect enough time − dependent deformation (creep) data for modeling the viscoelastic behavior. The uniaxial load (P) and specimen's longitudinal deformation versus time $\delta(t_i)$ were reported by the load frame at each 0.1 s. This information was used to calculate the specimen's true longitudinal strain ($\varepsilon(t_i)$) per Eq. (1), where (L_0) is the specimen's initial length. The true stress (Cauchy stress) versus time $\sigma(t_i)$ was also calculated per Eq. (2), where ν and r_0 are the Poisson's ratio and the initial radius of the specimen, respectively.

$$\varepsilon(t_i) = -ln\left(\frac{L_0}{L_0 - \delta(t_i)}\right) \tag{1}$$

$$\sigma(t_i) = \frac{P}{\pi r^2} = \frac{P}{\pi\left[r_0(1 - \nu\varepsilon(t_i))\right]^2} \cong \frac{0.4\sigma_c}{1 - 2\nu\varepsilon(t_i)} \quad \left[Note: \frac{P}{\pi r_0^2} = 0.4\sigma_c\right] \tag{2}$$

A close examination of the obtained strain − time curves for ASR gels suggested that they all have a common shape: an elastic (instantaneous) strain followed by a non − linear strain vs. time, leading to

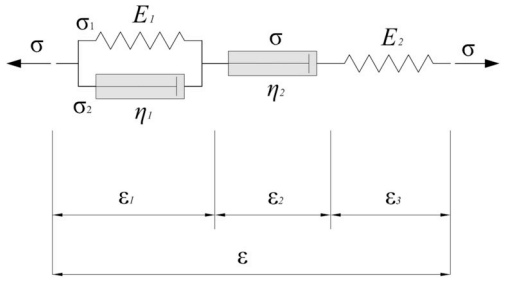

Fig. 2. Burgers model for characterizing the viscoelastic behavior of ASR gels.

a linear long − term strain vs. time (see Fig. 5). Among basic viscoelastic models, the Burgers model (Fig. 2) is capable of capturing such time − dependent strain response, and was used in the remaining of this study to model the viscoelastic behavior of ASR gels. The Burgers model has been also previously applied to model the time-dependent deformations in hydrogels [21] and hybrid organic and nonorganic composites [22].

2.2.6. Closed form solution of the burgers model

Before deriving a creep strain-time response based on the Burgers model, it is important to note that such rate constitutive equations should be written in an "objective" form to be valid. That is, the response of the material should be invariant under a change in the frame of observation. For instance, relating the Jaumman, Truesdell, or Green-Naghdi stress rates to the strain rate respects objectivity, as they take into consideration the effect of material rotation and produce a "frame-invariant" material response [23]. As an example, one can consider the Jaumman rate $\dot{\boldsymbol{\sigma}}_{\textbf{Jaumann}}$ of the true (Cauchy) stress, which can be expressed as:

$$\dot{\boldsymbol{\sigma}}_{\textbf{Jaumann}} = \frac{d\boldsymbol{\sigma}}{dt} - \boldsymbol{W}\cdot\boldsymbol{\sigma} - \boldsymbol{\sigma}\cdot\boldsymbol{W}^{\mathbf{T}} \tag{3}$$

where $\boldsymbol{\sigma}$ is the true stress tensor, $\frac{d\sigma}{dt}$ is the time-derivative of the true stress, $\boldsymbol{W} = \frac{1}{2}(\boldsymbol{L} - \boldsymbol{L}^{\boldsymbol{T}})$ is the spin tensor, and $\boldsymbol{L} = \partial\boldsymbol{v}/\partial\boldsymbol{x}$ is the velocity gradient.

However, it is critical to bear in mind that in the current experimental setup, each gel cylinder experienced only a uniaxial vertical stress, with no buckling, barreling, or rotation. The specimens responded by deforming/shortening uniformly in the vertical direction and expanding uniformly in the radial and tangential directions. Further, there was no strain gradient as every element within the specimen experienced the same magnitude of strain. Under these ideal conditions, no rotation occured within the material, yielding the fact that $\boldsymbol{W} = 0$, and the Jaumman rate is coincident with the time derivative of the true stress, that is, $\dot{\boldsymbol{\sigma}}_{\textbf{Jaumann}} = \frac{d\sigma}{dt}$. In other words, a normal time-derivative of true stress or true strain is objective [24] and can be used to derive frame-invariant constitutive equations.

To do so, according to the Burgers model (Fig. 2), the overall strain of a gel cylinder is considered as the sum of the strains in each of the three serial elements of the model (Eq. (4)).

$$\varepsilon(t) = \varepsilon_1(t) + \varepsilon_2(t) + \varepsilon_3(t) \tag{4}$$

While the spring elements follow the Hook's law, the dashpot elements follow the Newton's law of viscous flow. To find $\varepsilon_1(t)$, stress can be described as:

$$\sigma(t) = \sigma_1(t) + \sigma_2(t) = E_1.\,\varepsilon_1(t) + \eta_1.\,\frac{d\varepsilon_1(t)}{dt}$$
$$\Rightarrow \frac{d\varepsilon_1(t)}{dt} = \frac{\sigma(t)}{\eta_1} - \frac{E_1}{\eta_1}\varepsilon_1(t)$$

By solving the differential equation and applying the boundary conditions, $\varepsilon_1(t)$ is obtained per Eq. (5).

$$\varepsilon_1(t) = \frac{\sigma(t)}{E_1} - \frac{1}{E_1}\int_0^t \exp\left[-\frac{E_1}{\eta_1}.\,(t-u)\right]\dot{\sigma}(u).\,du \tag{5}$$

$\varepsilon_2(t)$ and $\varepsilon_3(t)$ can be easily shown to follow Eq. (6) and Eq. (7). By combining Eq. (4) to Eq. (7), it can be demonstrated that the total strain of a viscoelastic material obeying the Burgers model follows Eq. (8).

$$\varepsilon_2(t) = \frac{1}{\eta_2}.\int_0^t \sigma(u).\,du \tag{6}$$

$$\varepsilon_3(t) = \frac{\sigma(t)}{E_2} \tag{7}$$

Table 3
The viscoelastic parameters and Poisson's ratios of synthetic ASR gels.

Gel label	E_1 (MPa)	E_2 (MPa)	η_1 (MPa.s)	η_2 (MPa.s)	Poisson's ratio
$C^{II}N^{IH}K^{IH}$	91.2	20.1	1.72E+04	5.64E+04	0.084
$C^{II}N^{II}K^{IH}$	443	163	1.93E+05	2.55E+06	0.142
$C^{I}N^{L}K^{I}$	17600	525	3.41E+06	3.51E+07	0.081
$C^{II}N^{II}K^{IL}$	1574	210	3.99E+05	8.05E+05	0.128
$C^{H}N^{I}K^{I}$	659	223	7.67E+04	1.95E+06	0.09
$C^{I}N^{H}K^{I}$	24.25	16.5	5.11E+03	1.46E+05	0.117
$C^{I}N^{I}K^{I}$ (1)	191	68.7	3.29E+04	1.05E+06	0.159
$C^{IH}N^{II}K^{IH}$	668	210	1.52E+03	1.88E+04	0.497
$C^{IH}N^{IH}K^{IH}$	70	19.5	1.04E+04	4.72E+04	0.077
$C^{I}N^{I}K^{H}$	108	55.2	6.31E+03	4.06E+04	0.208
$C^{I}N^{I}K^{I}$ (2)	192	118	2.59E+04	9.96E+05	–
$C^{I}N^{I}K^{I}$ (3)	352	105	5.00E+04	8.85E+05	0.317
$C^{L}N^{I}K^{I}$	1.51	2.31	3.92E+02	3.83E+03	0.048
$C^{IH}N^{IH}K^{IL}$	117	55.6	9.68E+03	2.79E+05	0.258
$C^{I}N^{I}K^{I}$ (4)	266	154	6.77E+03	5.12E+05	0.192
$C^{II}N^{II}K^{IL}$	130	34.5	1.75E+04	3.99E+04	0.172
$C^{IH}N^{II}K^{IL}$	709	448	3.43E+04	3.17E+06	–
$C^{I}N^{I}K^{L}$	800	204	1.36E+05	4.08E+06	0.194

$$\varepsilon(t) = \sigma(t)\left(\frac{E_1 + E_2}{E_1E_2}\right) - \frac{1}{E_1}\int_0^t \exp\left[-\frac{E_1}{\eta_1}.\,(t-u)\right]\dot{\sigma}(u).\,du + \frac{1}{\eta_2}.\int_0^t \sigma(u).\,du \tag{8}$$

2.2.7. Regression analyses

Regressional analyses were performed for determining the values and confidence intervals of the viscoelastic parameters of the gels, and to link these with the chemical composition of the gels. The optimum E_1, E_2, η_1 and η_2 values were determined as those that minimized the difference between the experimentally observed strain values and those suggested per Eq. (8). Nonlinear Least Squares (nls) package of R software was used for fitting the strain function (Eq. (8)) to the strain − time data obtained for each gel. Details of the regression analyses are provided in Appendix A1. The results for E1, E2, η1 and η2 values of each gel is reported in Table 3.

After obtaining the experimental values for the compressive strength, Poisson's ratio, and viscoelastic parameters of the 18 synthetic gels (Table 3), separate regression analyses were conducted to model each parameter as a function of ASR gels' composition. Minitab software was used for such regression analyses. The significant predictors (including the linear, 2nd, and 3rd order terms, as well as the interactions between the composition variables) were identified and separate regression equations were developed for each response parameter.

2.2.8. The source of viscoelasticity in ASR gels

Before presenting the experimental and modeling results, it is worth considering the causes of viscoelasticity in ASR gels. The goal of this paper was to establish the composition-viscoelastic property relationships for ASR gels. Investigating the exact mechanisms of time-dependent deformation and establishing structure-property relationships for ASR gels is beyond the scope of the current paper and would be an excellent topic for a future research. However, here we offer general hypotheses to explain the possible causes of gel viscoelasticity.

ASR gel is composed of depolymerized silica sheets or particles that are held together by Van der Waals bonds [17]. These silica sheets are highly hygroscopic and hold both chemisorbed (i.e., silanol groups) and physisorbed water at their surface. In addition, the gel structure contains capillary/free water (Fig. 3). Under the applied stress, the gel's solid skeleton experiences some elastic deformation. This is represented by the parameter E_2 in the Burgers model (Fig. 2), which is referred to as the instant elastic modulus of ASR gels. In addition to this elastic response, all gels show significant time-dependent strains. Both the nonlinear and linear strain vs. time may be due to sliding and

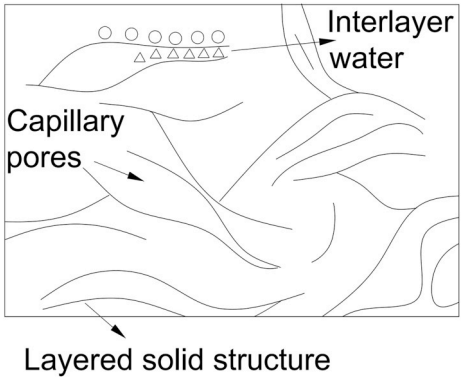

Fig. 3. 2 − D schematic diagram of the microstructure of ASR gel.

rearrangement of silica sheets under shear, induced by the external stress. This rearrangement is facilitated by the presence of water, as lubricant, between the silica sheets, and is similar to the mechanism of creep in concrete due to sliding of C–S–H sheets under stress [25]. Further, movement and seepage of capillary water and consolidation of the gel's solid structure can contribute to the strain development. Finally, the external stress can counter the disjoining pressure that exists between the silica sheets [22]. This results in diffusion of physisobed/interlayer water, which brings the silica sheets closer to each other and contributes to the overall time-dependent strain development. In the Burgers model, the parameters η_1 and E_1 (referred to as the nonlinear viscosity and modulus; see Fig. 2) account for the short − term nonlinear strain, while η_2 (the linear viscosity) represents the long − term linear strain evolution with time.

3. Results

3.1. Compressive strength

The uniaxial compressive strength test results are shown in Fig. 4. It is observed that depending on the gel composition, the compressive strength can be as low as 0.5 MPa (in the case of gel with low Ca/Si) or as high as 11.3 MPa (in the case of high Ca/Si or low Na/Si). For assessing the repeatability of this experiment, the compressive strength results of the replicates (i.e., $C^{I}N^{I}K^{I}$ (1) to (4)) were statistically analyzed. $C^{I}N^{I}K^{I}$ was found to have an average compressive strength of 6.27 MPa with a standard deviation of 1.19 MPa, which translated to a coefficient of variation equal to 19%.

3.2. Viscoelastic properties and Poisson's ratio results

Fig. 5 shows the time − dependent evolution of strain in the experimented ASR gel cylinders under a constant load as described earlier. Comparing the order of magnitude difference in the strain values developed in the gels at similar times suggests significant differences in the values of their viscoelastic properties. The strain − time results were analyzed following the protocol described in Appendix A1 to obtain the optimal values and 95% confidence intervals of different viscoelastic parameters of the gels, following the Burgers model. Table 3 shows E_1, E_2, η_1 and η_2 and Poisson's ratio results. Please refer to Appendix A2 for more information on the statistical details of these results. Using the results shown in Table 3 to regenerate the strain-time series of the gels, it was realized that the Burgers model with the fitted parameters is capable of predicting strain evolution over time with high precision.

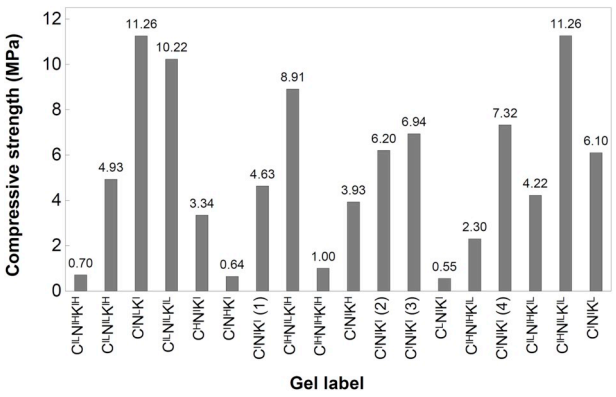

Fig. 4. The compressive strength results of the synthesized ASR gels.

It is also worth noting that all experimental observations were made by testing synthetic ASR gels at a constant solid concentration of 60% (water content of 40%). Had gels with higher solid concentrations been synthesized, greater values would be obtained for all viscoelastic parameters. However, producing gels with lower water contents was not practical using the synthesis method described earlier.

A preliminary inspection of the results in Table 3 suggest that an increase in Ca/Si and a decrease in Na/Si lead to increases in the elastic moduli and viscosity values of the gels. However, more in − depth quantitative characterization of the effects and interactions of Ca/Si, Na/Si, and K/Si on these parameters are needed, which requires statistical analysis and development of a regression model, which is carried out in section 4. Interestingly, all viscoelastic parameters of the gels show similar pattern of variations versus composition. Table 4 shows the Pearson correlation coefficients between E_1, E_2, η_1 and η_2. The p–values in all cases was found to be smaller than < 0.005. It is noted that all parameters have direct (positive) correlations.

The Poisson's ratio results in Table 3 show a wide range from 0.048 to as high as 0.497 depending on the gel composition. The accuracy of the maximum reading (for gel $C^{IH}N^{IL}K^{IH}$) is probably compromised because of an observed cracking and a disproportionate lateral expansion during the experiment, which is possibly due to the high Ca/Si and low Na/Si level of that specific gel. Moreover, considerable variations in the Poisson's ratio measurements were found for gels with similar compositions (e.g., $C^{I}N^{I}K^{I}$ (1) and $C^{I}N^{I}K^{I}$ (3)), which suggest that either the precision of the measurements or the repeatability of the method used for measuring the Poisson's ratio were not sufficient. As such, no further regression analyses on the Poisson's ratio results was carried out.

4. Regression models to establish composition-property relations

This section presents the results of separate regression analyses that were performed on the obtained results for the compressive strength and viscoelastic properties. The results for each response parameter were analyzed using Minitab software in order to quantify the effects and interactions of the chemical composition variables. The selected design of experiments allows for statistically assessing up to the 3rd order effects and the two–way interactions of the chemical variables.

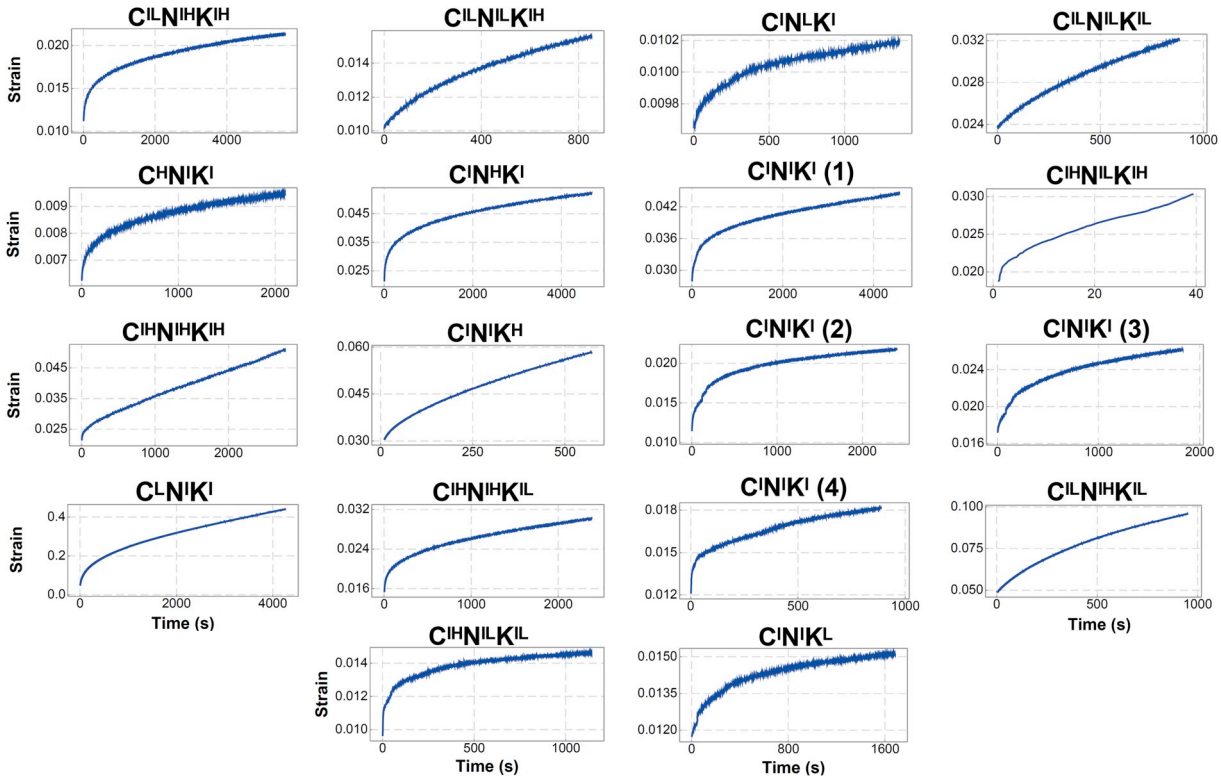

Fig. 5. The strain-time series of the experimented synthetic ASR gel cylinders under uniaxial constant load.

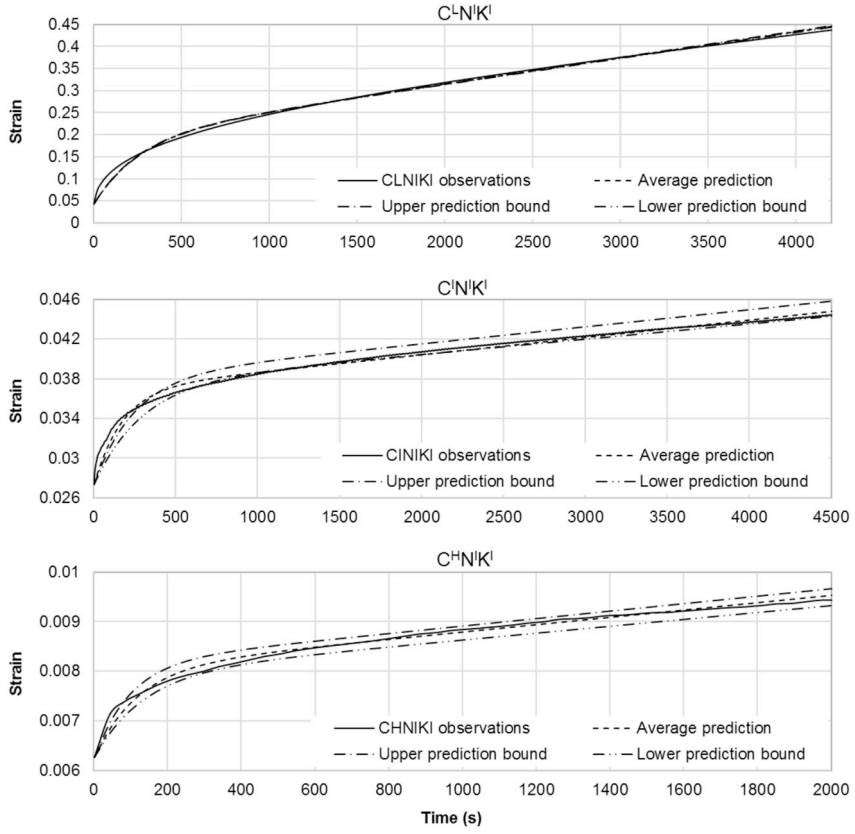

Fig. 6. The observed strain-time curves of $C^{L}N^{I}K^{I}$, $C^{I}N^{I}K^{I}$ and $C^{H}N^{I}K^{I}$ versus the average fitted values and.

Table 4
The Pearson correlation coefficients of different viscoelastic parameters.

Parameter	E_1	E_2	η_1
E_2	0.698		
η_1	0.998	0.677	
η_2	0.991	0.772	0.988

Table 5
The short–hand ANOVA table of ASR gels' compressive strength results.

Source	Coefficient	Contribution (%)	P − Value
Regression	–	93.19	0
Constant	7.14	–	–
Ca/Si	47.7	2.21	0.085
Na/Si	−5.91	68.22	0
K/Si	−28.1	8.77	0.003
$(Ca/Si)^2$	−70.1	9.90	0.002
Ca/Si × Na/Si	−23.3	2.56	0.067
Ca/Si × K/Si	54.1	1.53	0.144
Error	–	6.81	–
Lack − of − Fit	–	4.85	0.587
Pure Error	–	1.96	–
Coefficient of determination (R2 – %)	Regular 93.19	Adjusted 89.48	Predicted 80.34

4.1. Compressive strength

Table 5 shows the short–hand analysis of variance (ANOVA) table for the compressive strength results. Three quantities are reported in the ANOVA table; Contribution (%) to the total variations in the response, Coefficient of the predictor as it appears in the regression formula, and the p–value or the significance level of the predictor. A p–value smaller than 0.05 indicates a significant influence of the predictor on the response. Generally, the predictors with p–values considerably greater than 0.05 have been removed from the regression models unless their presence was needed for maintaining the hierarchy of the model or enhancing the coefficients of determination. For more information regarding the regression procedure and interpretation of the ANOVA table, the reader is referred to Refs. [12,26].

Using the ANOVA results per Table 5, the regression function for compressive strength can be constructed. The influencing sources of variations listed in the ANOVA table are multiplied by their corresponding coefficients and summed up in order to develop the regression equation. The resulting regression equation is shown as Eq. (9) below. As suggested by Table 5, the regression model has high coefficients of determination (R^2). The regular R^2 was found to be 93.19% and the predicted R^2 (which is a measure of the model's accuracy in predicting new observations) is 80.34%. The obtained R^2 values are indicative of the model's high accuracy in predicting the existing and new experimental results on the compressive strength of ASR gels as a function of their composition.

$$\sigma_c(MPa) = 7.14 + 47.7\left(\frac{Ca}{Si}\right) - 5.91\left(\frac{Na}{Si}\right) - 28.1\left(\frac{K}{Si}\right) - 70.1\left(\frac{Ca}{Si}\right)^2 - 23.3\left(\frac{Ca}{Si}\right)\left(\frac{Na}{Si}\right) + 54.1\left(\frac{Ca}{Si}\right)\left(\frac{K}{Si}\right) \quad (9)$$

The obtained regression equation can be graphically illustrated in Fig. 7. 7a shows the sole effects of each composition variable (i.e., Ca/Si, Na/Si and K/Si) on the compressive strength of ASR gels, where the other two variables are held constant at their intermediate levels per Table 1 (e.g., Na/Si = 0.55 and K/Si = 0.15 in the case of the graph showing the effect of Ca/Si on gel compressive strength). It is observed that higher alkali contents drastically reduce the compressive strength of gels, while Ca/Si has a 2nd order effect causing increase in the compressive strength up to $(Ca/Si)_{opt} = 0.31$, followed by a reducing effect. Among all variables, Na/Si has by far the largest contribution to the variations observed in the compressive strength of the gels.

Marginally significant two − way interactions were found between Ca/Si and Na/Si (P–Value = 0.067), and also between Ca/Si and K/Si (P–Values = 0.144, suggesting 14.4% chance for lack of statistical significance). As such, it is reasonable to plot the effect of Ca/Si on compressive strength at different levels of Na/Si and K/Si to obtain a better visualization of the effect of Ca/Si on strength. Fig. 7b and 7c shows the interactions between Ca/Si and Na/Si, and Ca/Si and K/Si, respectively. It is observed that at low values of Na/Si or K/Si, the effect of Ca/Si on the compressive strength is more pronounced. On the other hand, at high Na/Si, Ca/Si does not significantly affect the compressive strength (Fig. 7b).

4.2. Viscoelastic properties

The four viscoelastic parameters were statistically modeled using the Minitab software. The regression analyses results are shown in Table 6. The results suggest that Ca/Si has generally promoting (increasing) effects on all of the viscoelastic parameters of the gels, while increase in Na/Si and K/Si always lead to a decrease in these parameters. It should be noted that all viscoelastic parameters in Table 6 have been transformed to some power or natural log. This step, known as the Box–Cox transformation, is taken in order to eliminate the heteroscedasticity of the prediction errors (i.e., variation in the variance of prediction errors across different observations which is a violation of the core assumptions of the regression analysis).

The "Coef." columns in Table 6 show the coefficients for each predictor (e.g., Ca/Si × Na/Si) in the regression equation fitted to each viscoelastic parameter. For example, the regression equation describing E_1 (nonlinear modulus) can be written per Eq. (10):

$$\{E_1(MPa)\}^{0.1} = 2.038 + 15.90\left(\frac{Ca}{Si}\right) - 7.03\left(\frac{Na}{Si}\right) - 0.817\left(\frac{K}{Si}\right) - 57.34\left(\frac{Ca}{Si}\right)^2 . + 10.93\left(\frac{Na}{Si}\right)^2 + 63.33\left(\frac{Ca}{Si}\right)^3 - 5.784\left(\frac{Na}{Si}\right)^3 \quad (10)$$

This equation can be graphically illustrated in Fig. 8, which shows the effects of Ca/Si, Na/Si and K/Si, and their interactions on the fitted E_1 per the proposed regression equation. It is observed that alkalis (especially Na/Si) have reducing effects on E_1 while Ca/Si has a generally promoting effect on E_1. Similar to E_1, no significant interactions between the chemical variables were observed in the case of E_2. The main influence of the gel's composition variables on E_2 were otherwise similar to those effects on E_1. The main effects and interaction plots for η_1 and η_2 were also analogous to those of E_1 and as such, are not plotted independently in this paper.

Fig. 9 shows the contour plots of E_1 (plots (a) through (c)) and E_2 (plots (d) through (f)) with respect to the composition variables Ca/Si, Na/Si, and K/Si. Each contour plot assumes two of the three composition components as variables while the third one is held constant at its intermediate level. For instance, Fig. 9a is the contour plot of E_1 versus Ca/Si and Na/Si where K/Si is held constant at 0.15. All figures confirm the previous observations regarding the effects of gel composition on its viscoelastic properties. While Na/Si and K/Si monotonically and significantly reduce the gel stiffness parameters E_1 and E_2, Ca/Si has a cubic effect in the direction of increasing E_1 and E_2. It is noted that the greyed area on each graph represents the area that is outside the DoE domain. Caution must be exercised when using these contour plots in such grey regions as it amounts to an extrapolation using the regression equations.

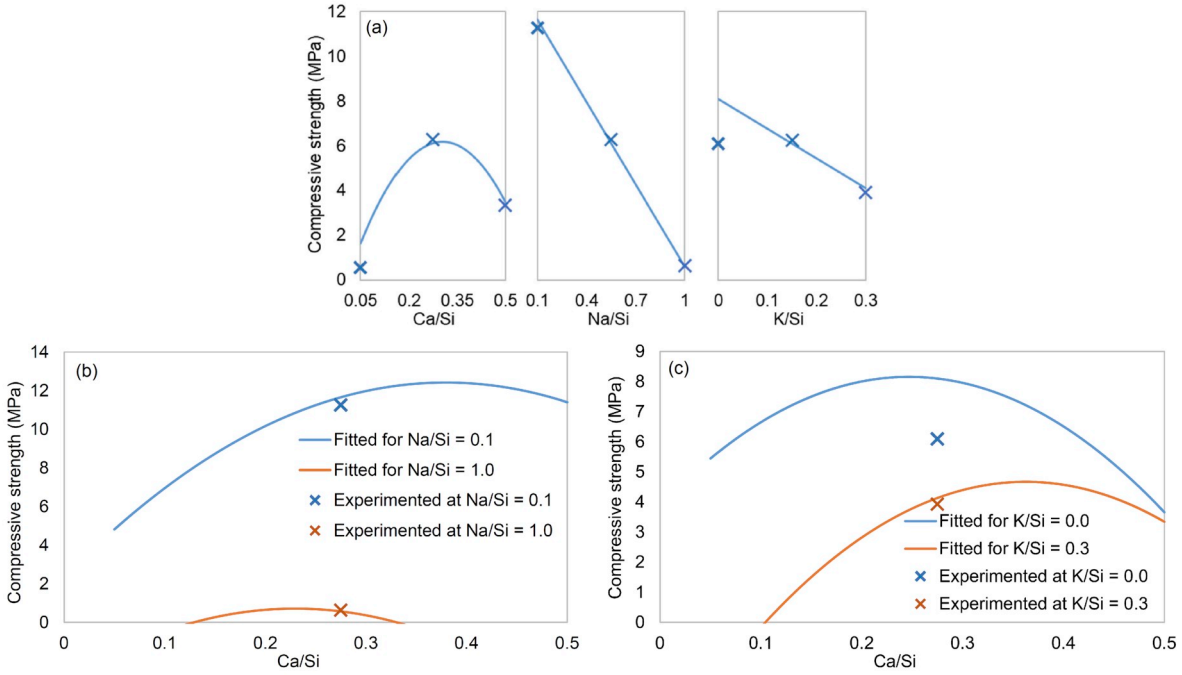

Fig. 7. The main effects and interactions plots of gel compressive strength with respect to the composition variables; the curves show the mean fitted values per the regression function; the corresponding experimental results are shown by cross markers.

Table 6
The short–hand ANOVA table of ASR gels' viscoelastic parameters.

Response	$\{E_1$ (MPa)$\}^{0.1}$			$\{E_2$ (MPa)$\}^{0.15}$			Ln$\{\eta_1$ (MPa.s)$\}$			$\{\eta_2$ (MPa.s)$\}^{-0.258}$		
Predictor	Cont. (%)	Coef	P − Val	Cont. (%)	Coef.	P − Val	Cont. (%)	Coef.	P − Val	Cont. (%)	Coef	P − Val
Constant	–	2.038	0.000	–	1.280	0.000	–	13.15	0.001	–	−0.195	0.000
Ca/Si	6.88	15.90	0.000	17.43	16.83	0.000	0.02	123.0	0.886	10.73	2.059	0.000
Na/Si	50.63	−7.030	0.000	55.56	−1.146	0.000	24.68	−48.3	0.001	10.45	−0.070	0.000
K/Si	3.88	−0.817	0.000	6.33	−1.163	0.000	7.91	−7.36	0.020	12.10	0.439	0.000
$(Ca/Si)^2$	8.57	−57.34	0.000	6.94	−57.63	0.000	8.24	−525.9	0.018	21.08	−6.743	0.000
$(Na/Si)^2$	7.02	10.93	0.000	–	–	–	5.38	70.1	0.045	–	–	–
$(K/Si)^2$	–	–	–	–	–	–	–	–	–	1.93	−0.535	0.007
Ca/Si × Na/Si	–	–	–	–	–	–	6.48	21.60	0.031	5.02	0.028	0.000
Ca/Si × K/Si	–	–	–	–	–	–	–	–	–	8.91	−1.785	0.000
Na/Si × K/Si	–	–	–	–	–	–	–	–	–	1.09	−0.228	0.025
$(Ca/Si)^3$	13.64	63.33	0.000	10.70	62.51	0.000	30.57	599	0.000	26.36	7.186	0.000
$(Na/Si)^3$	7.28	−5.784	0.000	–	–	–	7.82	−37.8	0.020	–	–	–
$(K/Si)^3$	–	–	–	–	–	–	–	–	–	–	–	–
Ca/Si × Na/Si × K/Si	–	–	–	–	–	–	–	–	–	1.39	1.454	0.015
Error	2.10	–		3.03	–		8.90	–		0.95	–	–
Lack − of − Fit	1.62	–	0.413	1.71	–	0.855	5.42	–	0.638	0.76	–	0.190
Pure Error	0.48	–		1.32	–		3.48	–		0.18	–	–
Coefficient of determination (R^2 – %)	Reg.	Adj.	Pred	Reg.	Adj.	Pred.	Reg.	Adj.	Pred.	Reg.	Adj.	Pred
	97.90	96.43	93.23	96.97	95.71	83.96	91.10	83.19	71.51	99.05	97.70	84.07

5. Conclusions and future work

ASR gels of various compositions were synthesized and tested using a simple uniaxial compression setup under constant load. In this setup, the viscoelastic properties of ASR gels could be well characterized using the Burgers model. It was observed that the modulus and viscosity parameters (E_1, E_2, η_1, and η_2) as well as the uniaxial compressive strength of the gels were all highly correlated with the composition of the gels, namely, their Ca/Si, Na/Si and K/Si molar ratios. Based on a statistical design of experiments (DoE), regression equations were established to predict the viscoelastic parameters with known reliability. It was observed that an increase in the gels' alkali content (Na + K)/Si led to drastic decline in the stiffness (moduli) and viscosity of the gels. Meanwhile, Ca/Si generally increased the stiffness and viscosity in a nonlinear manner. Possible explanations for the observed behaviors were proposed.

Further research is needed to identify how the gel microstructure evolves for different gel compositions, and how such microstructural arrangements impact the mechanical and swelling properties of ASR gels. Also, research into better identifying the mechanisms responsible for the viscoelastic response of ASR gels is recommended. It is helpful to perform similar experiments using a tri-axial or other stress configurations and at different stress levels to verify the linear creep assumption and to better replicate the real state of stress and strain experienced by ASR gels inside concrete. In this regard, it is important to account for the effects of confining stress on the viscoelastic parameters, and to develop a more advanced viscoelastic model that ensures objectivity under complex stress and strain configurations.

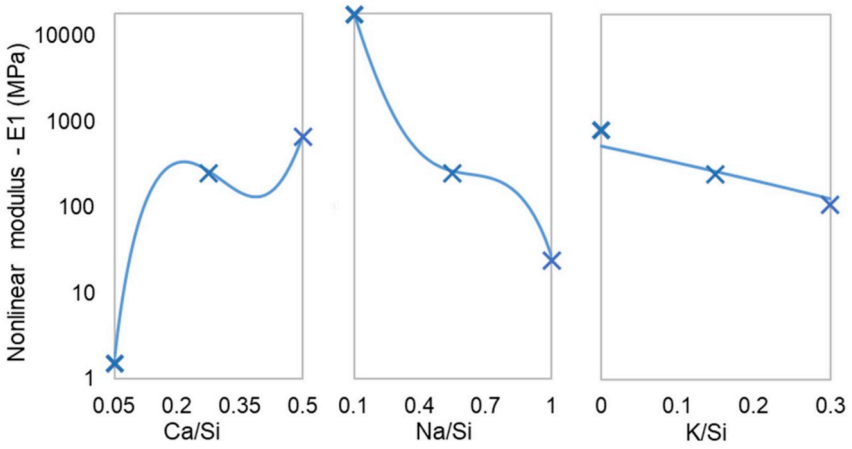

Fig. 8. The main effects plots of the gel nonlinear modulus (E_1) with respect to chemical variables; the curves show the mean fitted values per the regression function; the corresponding experimental results are shown by cross markers.

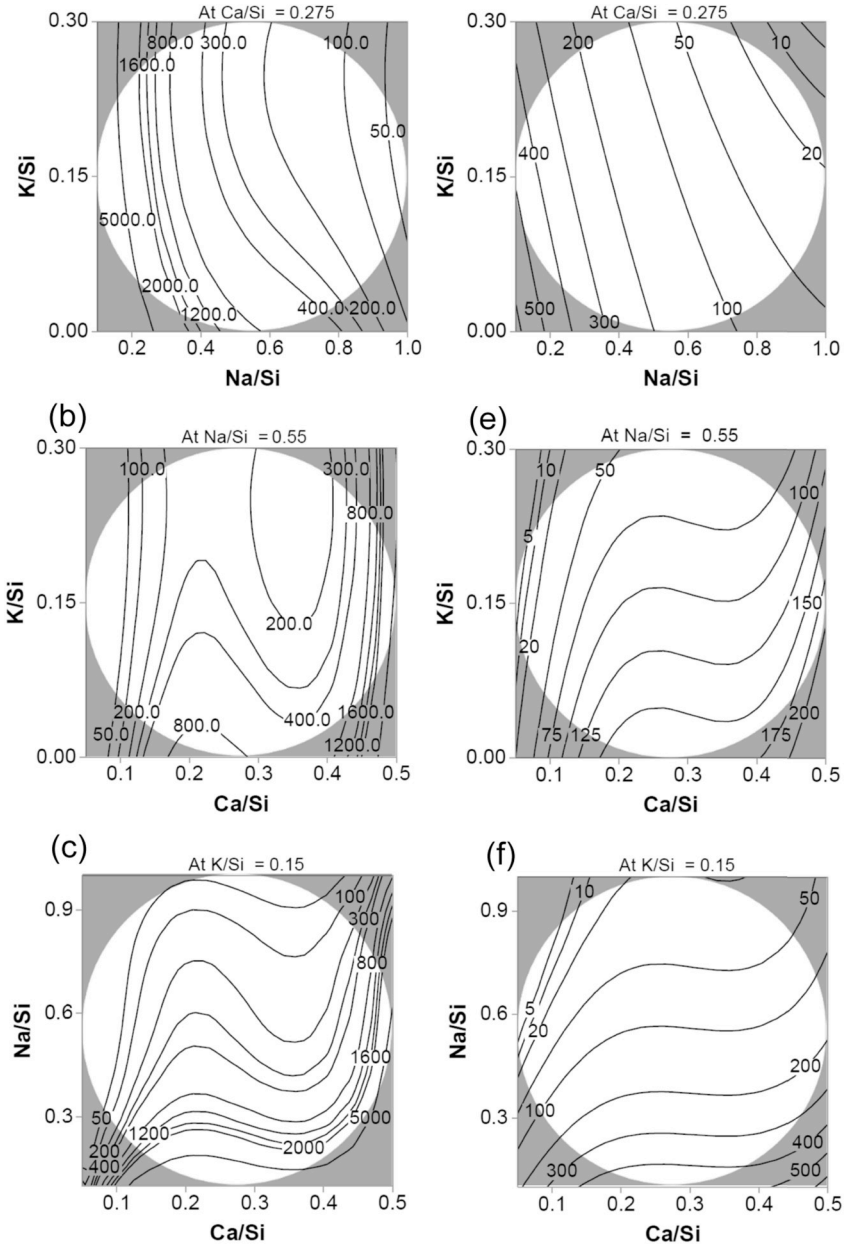

Fig. 9. The contour plots of the elastic moduli of ASR gels according to the Burgers model: (a)–(c) nonlinear modulus: E_1, (d)–(f) instant modulus: E_2.

Acknowledgements

The authors gratefully acknowledge the financial support from the U.S. National Science Foundation (NSF) under CMMI CAREER Award# 1254333, awarded to the second author. Any opinions, findings, conclusions, or recommendations expressed in this manuscript are those of the authors solely and do not necessarily reflect the views of NSF. The invaluable experimental support of Mr. Dan Fura is greatly appreciated. The first author would like to dedicate this work to his family and especially his mother for their constant support and encouragements, which made this work possible.

Appendix A. Supplementary data

Supplementary data to this article can be found online at https://doi.org/10.1016/j.cemconcomp.2019.103359.

References

[1] F. Pesavento, D. Gawin, M. Wyrzykowski, B.A. Schrefler, L. Simoni, Modeling alkali–silica reaction in non-isothermal, partially saturated cement based materials, Comput. Methods Appl. Mech. Eng. 225 (2012) 95–115.
[2] F.J. Ulm, O. Coussy, L. Kefei, C. Larive, Thermo-chemo-mechanics of ASR expansion in concrete structures, J. Eng. Mech. 126 (3) (2000) 233–242.
[3] C.F. Dunant, K.L. Scrivener, Micro-mechanical modelling of alkali–silica-reaction-induced degradation using the AMIE framework, Cement Concr. Res. 40 (4) (2010) 517–525.
[4] A.B. Giorla, K.L. Scrivener, C.F. Dunant, Influence of visco-elasticity on the stress development induced by alkali–silica reaction, Cement Concr. Res. 70 (2015) 1–8.
[5] S. Multon, A. Sellier, M. Cyr, Chemo–mechanical modeling for prediction of alkali silica reaction (ASR) expansion, Cement Concr. Res. 39 (6) (2009) 490–500.
[6] W. Xu, Calculation of alkali silica reaction (ASR) induced expansion before cracking of concrete, J. Wuhan Univ. Technol.-Materials Sci. Ed. 28 (1) (2013) 110–116.
[7] A.S. Kodjo, P. Rivard, F. Cohen-Tenoudji, J.L. Gallias, Impact of the alkali–silica reaction products on slow dynamics behavior of concrete, Cement Concr. Res. 41 (4) (2011) 422–428.
[8] Z.P. Bažant, A. Steffens, Mathematical model for kinetics of alkali–silica reaction in concrete, Cement Concr. Res. 30 (3) (2000) 419–428.
[9] J.H. Ideker, A.F. Bentivegna, K.J. Folliard, M.C.G. Juenger, Do current laboratory test methods accurately predict alkali-silica reactivity? ACI Mater. J. 109 (4) (2012) 395–402.
[10] A. Gholizadeh-Vayghan, F. Rajabipour, The influence of alkali–silica reaction (ASR) gel composition on its hydrophilic properties and free swelling in contact with water vapor, Cement Concr. Res. 94 (2017) 49–58.
[11] A. Gholizadeh-Vayghan, F. Rajabipour, Quantifying the swelling properties of alkali-silica reaction (ASR) gels as a function of their composition, J. Am. Ceram. Soc. 100 (2017) 3801–3818.
[12] A. Gholizadeh Vayghan, F. Rajabipour, J.L. Rosenberger, Composition–rheology relationships in alkali–silica reaction gels and the impact on the Gel's deleterious behavior, Cement Concr. Res. 83 (2016) 45–56.
[13] C.F. Dunant, K.L. Scrivener, Physically based models to study the alkali–silica reaction, Proc. Inst. Civ. Eng. Constr. Mater. 169 (3) (2016) 136–144.
[14] J.W. Phair, S.N. Tkachev, M.H. Manghnani, R.A. Livingston, Elastic and structural properties of alkaline-calcium silica hydrogels, J. Mater. Res. 20 (02) (2005) 344–349.
[15] M.J. Murtagh, E.K. Graham, C.G. Pantano, Elastic moduli of silica gels prepared with tetraethoxysilane, J. Am. Ceram. Soc. 69 (11) (1986) 775–779.
[16] A. Leemann, P. Lura, E-modulus of the alkali–silica-reaction product determined by micro-indentation, Constr. Build. Mater. 44 (2013) 221–227.
[17] F. Rajabipour, E. Giannini, C. Dunant, J.H. Ideker, M.D. Thomas, Alkali–silica reaction: current understanding of the reaction mechanisms and the knowledge gaps, Cement Concr. Res. 76 (2015) 130–146.
[18] M. Thomas, The role of calcium hydroxide in alkali recycling in concrete, Mater. Sci. Concr. Spec. (2001) 225–236.
[19] X. Hou, R.J. Kirkpatrick, L.J. Struble, P.J. Monteiro, Structural investigations of alkali silicate gels, J. Am. Ceram. Soc. 88 (4) (2005) 943–949.
[20] D.C. Montgomery, Design and Analysis of Experiments, John Wiley & Sons, 2008.
[21] M. Gasik, A. Gantar, S. Novak, Viscoelastic behaviour of hydrogel-based composites for tissue engineering under mechanical load, Biomed. Mater. 12 (2) (2017) 025004.
[22] S.B. Adalja, J.U. Otaigbe, Creep and recovery behavior of novel organic-inorganic polymer hybrids, Polym. Compos. 23 (2) (2002) 171–181.
[23] T. Belytschko, W.K. Liu, B. Moran, K.I. Elkhodary, Nonlinear Finite Elements for Continua and Structures, Sec. 3.7.2: Objective Rates in Constitutive Equations, second ed., Wiley, West Sussex, UK, 2014.
[24] G.A. Holzapfel, Nonlinear Solid Mechanics. A Continuum Approach for Engineering, Wiley, Chichester, 2000.
[25] S. Mindess, J.F. Young, D. Darwin, Concrete, Sec. 16.4: Creep of Concrete, second ed., Prentice Hall, New Jersey, USA, 2003.
[26] J. Neter, M.H. Kutner, C.J. Nachtsheim, W. Wasserman, Applied Linear Statistical Models, fourth ed., Irwin, Chicago, USA, 1996, p. 318.